

Technical note: Discharge response of a confined aquifer with variable thickness to temporal nonstationary random recharge processes

Ching-Min Chang¹, Chuen-Fa Ni¹, We-Ci Li¹, Chi-Ping Lin², and I-Hsian Lee²

¹Graduate Institute of Applied Geology, National Central University, Taoyuan, Taiwan

²Center for Environmental Studies, National Central University, Taoyuan, Taiwan

Correspondence: Chuen-Fa Ni (nichuenfa@geo.ncu.edu.tw)

1 **Abstract.** This work develop a transfer function to describe the variation of the
2 integrated specific discharge in response to the temporal variation of the rainfall event
3 in the frequency domain. It is assumed that the rainfall-discharge process takes place in
4 a confined aquifer with variable thickness, and it is treated as nonstationary in time to
5 represent the stochastic nature of the hydrological process. The presented transfer
6 function can be used to quantify the variability of the integrated discharge field
7 induced by the variation of rainfall field or to simulate the discharge response of the
8 system to any varying rainfall input at any time resolution using the convolution model.
9 It is shown that with the Fourier-Stieltjes representation approach a closed-form
10 expression for the transfer function in the frequency domain can be obtained, which
11 provide a basis for the analysis of the influence of controlling parameters occurring in
12 the rainfall rate and integrated discharge models on the transfer function.

13

14 **1 Introduction**

15

16 Quantifying the variability of specific discharge response of an aquifer system to
17 fluctuations in inflow recharge is essential for efficient groundwater resources
18 management. However, this requires extensive and continuous hydrological
19 time-series data, and these data are very often not available in practice. One possible

20 approach (namely, convolution or transfer function approach) to this problem is to
21 simulate the discharge response by convolution of the time-varying recharge input
22 with the corresponding impulse response. In convolution models, the aquifer is
23 regarded as a filter that converts recharge signals into fluctuations of the aquifer head
24 or discharge. Lumped conceptual-convolution models have been shown to be an
25 efficient means for the simulation of time series of groundwater levels (e.g., Gelhar,
26 1974; Molénat et al., 1999; Olsthoorn, 2007; Long and Mahler, 2013; Pedretti et al.,
27 2016).

28 Since the impulse response function in the convolution model contains all
29 information of the system necessary to relate its input to its output, it may be
30 determined from the analytical solution of the linear system equation governing the
31 input-output process (e.g., Cooper and Rorabaugh, 1963). Once a suitable impulse
32 response function can be specified, it allows the simulation of the linear system
33 response to any varying input at any time resolution.

34 In this work, a regional-scale flow in a confined aquifer with variable thickness,
35 which is recharged by rainfall through an outcrop, is analyzed by deriving transfer
36 functions to characterize the rainfall-discharge process in the frequency domain. The
37 stochastic analysis of groundwater flow is traditionally based on the assumption of
38 stationarity of the recharge and discharge processes. However, the hydrologic process

39 in nature is nonstationary-stochastic (e.g., Christensen and Lettenmaier, 2007; Milly
40 et al., 2008; Sang et al., 2018). In order to improve the quantification of the natural
41 recharge-discharge process, the nonstationary rainfall-discharge process is assumed in
42 this study. The Fourier-Stieltjes representation approach is used to achieve the goal of
43 this work. The analysis of the results is focused on the influence of controlling
44 parameters in the rainfall-discharge models on the transfer function.

45

46 **2 Problem formulation**

47

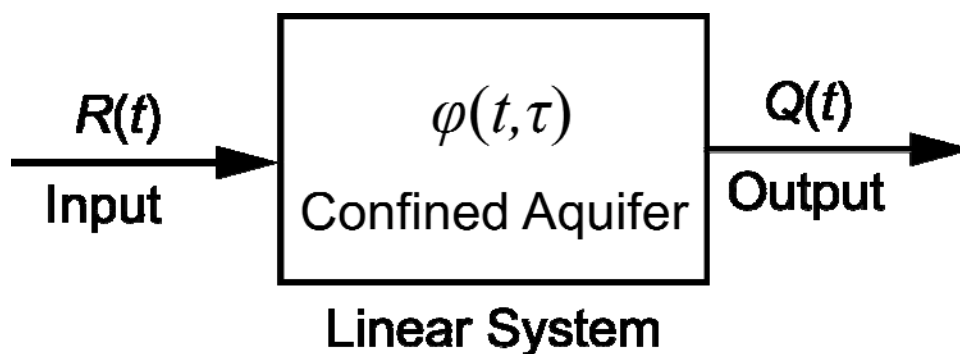
48 In certain areas, aquifer recharge can vary greatly over time, so determining the
49 discharge of the aquifer at the outlet for regional groundwater problems, which
50 involves transferring recharge at the aquifer outcrop over a relatively large space scale,
51 can be quite difficult. However, it is very important for planning and management of
52 regional groundwater resources that require knowledge of discharge at the aquifer
53 outlet over a long period of time. This study is therefore devoted to quantifying the
54 discharge response of the confined aquifer at the outlet to the temporal variation in
55 aquifer recharge.

56 In this study, a confined aquifer with variable thickness is considered as a linear
57 block-box system with a stochastic rainfall recharge input and therefore a stochastic

58 runoff output. Both inputs and outputs are variable in time. In a linear system, the
 59 output of the system can be represented as a linear combination of the responses to
 60 each of the basic inputs through the convolution integral on a continuous time scale as
 61 (e.g., Rugh, 1981; Rinaldo and Marani, 1987)

$$62 \quad Q(t) = \int_0^t \varphi(t, \tau) R(\tau) d\tau, \quad (1)$$

63 where Q and R denote the output flow (discharge) rate and the input flow (recharge)
 64 rate of the system, respectively, and φ is the impulse response function of the system.
 65 As shown in Fig. 1, once an appropriate impulse response function can be specified at
 66 the scale of the aquifer, it is possible to evaluate the system response from records of
 67 the input without the need to specify smaller scale heterogeneity. As will be shown
 68 below, the transfer function of the system can be used to characterize the uncertainty
 69 (variability) expected in applying the convolution integral Eq. (1) to the regional
 70 groundwater flow problems.



71

72 **Figure 1.** Schematic representation of a linear block-box system.

73 When using the nonstationary Fourier-Stieltjes representations for the perturbed

74 quantities of random recharge and outflow discharge processes, namely (e.g.,
 75 Priestley, 1965)

$$76 \quad r(t) = R(t) - E[R(t)] = \int_{-\infty}^{\infty} A_r(t; \omega) dZ_{\xi}(\omega), \quad (2)$$

$$77 \quad q(t) = Q(t) - E[Q(t)] = \int_{-\infty}^{\infty} A_q(t; \omega) dZ_{\xi}(\omega), \quad (3)$$

78 the power spectrum of the mean-removed convolution (1) can be written in the form

$$79 \quad S_{qq}(t; \omega) = \left| A_q(t; \omega) \right|^2 S_{\xi\xi}(\omega), \quad (4)$$

80 where

$$81 \quad A_q(t; \omega) = \int_0^t \varphi(t, \tau) A_r(\tau; \omega) d\tau. \quad (5)$$

82 In Eqs. (2) and (3), A_r and A_q are the oscillatory functions (Priestley, 1965) of the
 83 recharge and outflow processes, respectively, ω is the frequency, ξ is a zero-mean
 84 random stationary forcing process, which generates the variations of the recharge and
 85 thus the output flow processes, with an orthogonal increment dZ_{ξ} . In Eq. (4), S_{qq} and
 86 $S_{\xi\xi}$ represent the power spectra of the processes q and ξ , respectively, and $|A_q|^2$ is
 87 termed the transfer function.

88 In practice, the interest in many cases resides in evaluating the influence of the
 89 variation of recharge on the variation of the outflow discharge. Equation (4) provides
 90 an efficient way to quantify the variability of the outflow induced by the fluctuations
 91 of the inflow process in the frequency domain, since it relates the fluctuations of an

92 output time series to those of an input series.

93 It is worthwhile to mention that for the case of second-order stationary rainfall
94 processes, the representations of the forms (2) and (3) are reduced, respectively, to

$$95 \quad r(t) = \int_{-\infty}^{\infty} e^{i\omega t} dZ_r(\omega), \quad (6)$$

$$96 \quad q(t) = \int_{-\infty}^{\infty} A_q(t; \omega) dZ_r(\omega), \quad (7)$$

97 and correspondingly

$$98 \quad S_{qq}(t; \omega) = |A_q(t; \omega)|^2 S_{rr}(\omega), \quad (8)$$

99 where

$$100 \quad A_q(t; \omega) = \int_0^t \varphi(t, \tau) e^{i\omega \tau} d\tau. \quad (9)$$

101 Equations (1) and (4) reveal that once the transfer function for the linear lumped
102 system is identified, the first two moments of temporal random discharge fields can be
103 determined. That is, the transfer function approach provides a basic framework for the
104 characterization of large-scale flow processes, which may serve as a basis for an
105 efficient management of groundwater resources. Furthermore, Eq. (4) provides
106 another possible way to identify the aquifer parameters, as it relates the observed
107 fluctuations of an output discharge process to those of a recharge process in the
108 frequency domain.

109 In the following, the focus is on the development of a closed-form expression for

110 the transfer function for a linear lumped confined flow model, in which the regional
111 confined aquifer is directly recharged by rainfall in the area corresponding to the high
112 elevation outcrop.

113

114 **3 Theoretical development**

115

116 The differential equation describing the transient flow of groundwater in
117 inhomogeneous isotropic confined aquifers is of the form (e.g., Bear, 1979; de
118 Marsily, 1986)

$$119 \quad S_s \frac{\partial}{\partial t} h(\mathbf{x}, t) = \frac{\partial}{\partial x_i} \left[K(\mathbf{x}) \frac{\partial}{\partial x_i} h(\mathbf{x}, t) \right] \quad i = 1, 2, 3, \quad (10)$$

120 in which S_s represents the specific storage coefficient of the aquifer, $h = h(\mathbf{x}, t)$ is the
121 hydraulic head, $K(\mathbf{x})$ is the hydraulic conductivity, and $\mathbf{x} (= (x_1, x_2, x_3))$ is the spatial
122 coordinate vector. Many problems of groundwater flow are regional in nature, with
123 the horizontal extent of the formation being much larger than the vertical extent. It is
124 more practical to regard the flow as essentially horizontal. The regional-scale flow
125 equations can be derived by integrating Eq. (10) along the thickness of the confined
126 aquifer using the assumption of vertical equipotential surfaces (e.g., Bear, 1979; Bear
127 and Cheng, 2010).

128 Integrating Eq. (10) along the x_3 -axis perpendicular to the confining beds and

129 using Leibnitz' rule results in

$$130 \quad S(x_1, x_2) \frac{\partial}{\partial x_i} \tilde{h}(x_1, x_2, t) = \frac{\partial}{\partial x_i} \left[T(x_1, x_2) \frac{\partial}{\partial x_i} \tilde{h}(x_1, x_2, t) \right] + T(x_1, x_2) \frac{\partial}{\partial x_i} \ln B(x_1, x_2) \frac{\partial}{\partial x_i} \tilde{h}(x_1, x_2, t), \quad i = 1, 2 \quad (11)$$

131 where $S(x_1, x_2)$ is the storage coefficient (or storativity) of the aquifer ($= S_s B(x_1, x_2)$),

132 $B(x_1, x_2) = b_2(x_1, x_2) - b_1(x_1, x_2)$ (an aquifer's thickness), $b_1(x_1, x_2)$ and $b_2(x_1, x_2)$ are the

133 elevations of the fixed bottom and ceiling of the confined aquifer, respectively, $T(x_1, x_2)$

134 is the transmissivity of the aquifer ($= K(x_1, x_2) B(x_1, x_2)$), interpreted as the

135 depth-integrated hydraulic conductivity, and $\tilde{h}(x_1, x_2, t)$ is the depth-averaged

136 hydraulic head defined as

$$137 \quad \tilde{h}(x_1, x_2) = \frac{1}{b_2(x_1, x_2) - b_1(x_1, x_2)} \int_{b_1(x_1, x_2)}^{b_2(x_1, x_2)} h(x_1, x_2, x_3, t) dx_3, \quad (12)$$

138 Equation (11) is derived under the following assumptions: (1) there is no exchange of

139 leakage fluxes between the confined aquifer and its confining beds in the direction of

140 x_3 -axis, (2) $h(x_1, x_2, b_2, t) \approx \tilde{h}(x_1, x_2, t) \approx h(x_1, x_2, b_1, t)$ (vertical equipotentials; Bear,

141 1979; Bear and Cheng, 2010), and (3) all terms involved in the fluxes in the directions

142 of x_1 and x_2 at the boundaries are removed due to the no-slip condition at the

143 boundaries.

144 The use of the depth-averaged hydraulic head operator for modeling regional

145 groundwater flow is valid when the variation in aquifer thickness is much smaller

146 than the average thickness (Bear, 1979; Bear and Cheng, 2010). The error

147 introduced by the use of this operator is very small in most cases of practical

148 interest, greatly simplifying the analysis of flow in confined aquifers.

149 Similarly, when applying Leibnitz' rule to Darcy equation, the vertically
150 integrated specific discharge in the x_i direction is given by

$$151 \quad Q_{x_i}(x_1, x_2, t) = -K(x_1, x_2)B(x_1, x_2) \frac{\partial}{\partial x_i} \tilde{h}(x_1, x_2, t) = -T(x_1, x_2) \frac{\partial}{\partial x_i} \tilde{h}(x_1, x_2, t). \quad i = 1, 2 \quad (13)$$

152 In this study, the regional confined aquifer is considered with a nonuniform,
153 unidirectional mean flow in the x_1 -axis direction, but with small flow variations in the
154 x_1 - and x_2 -axis directions and time-varying recharge at the aquifer outcrop ($x_1 = 0$).

155 Since the regional flow domain considered in the x_1 direction is much larger than that in
156 the x_2 direction, Eqs. (11) and (13) can be approximated as one-dimensional by

$$157 \quad \frac{S(x)}{\bar{T}} \frac{\partial}{\partial t} \tilde{h}(x, t) = \frac{\partial^2}{\partial x^2} \tilde{h}(x, t) + \frac{\partial}{\partial x} \ln \bar{T}(x) \frac{\partial}{\partial x} \tilde{h}(x, t) + \frac{\partial}{\partial x} \ln B(x) \frac{\partial}{\partial x} \tilde{h}(x, t) + \frac{R(t)}{\bar{T}}, \quad (14)$$

$$158 \quad Q_x(x, t) = -\bar{T}(x) \frac{\partial}{\partial x} \tilde{h}(x, t), \quad (15)$$

159 where $\bar{T} = \bar{K}B$, \bar{K} represents the spatial average of the hydraulic conductivity,
160 and R is the recharge rate. It is worth noting that a one-dimensional flow equation

161 with the transmissivity parameter has been widely used to predict the regional
162 groundwater flow fields in the downstream region of the aquifer in field applications

163 (e.g., Gelhar, 1974; Onder, 1998; Molénat et al., 1999; Russian et al., 2013). Equation

164 (14) can be expressed alternatively as

$$165 \quad \frac{S_s}{K} \frac{\partial}{\partial t} \tilde{h}(x, t) = \frac{\partial^2}{\partial x^2} \tilde{h}(x, t) + 2 \frac{\partial}{\partial x} \ln B(x) \frac{\partial}{\partial x} \tilde{h}(x, t) + \frac{R(t)}{KB(x)}. \quad (16)$$

166 for the convenient analysis of the effect of the thickness of the aquifer.

167 In the following analysis, the recharge rate is considered a random function of
 168 time. Equation (15) is then regarded as a stochastic differential equation with a
 169 stochastic input in time and therefore a stochastic output in time. Introduction of
 170 decomposition of the depth-averaged hydraulic head into a mean and a zero-mean
 171 perturbation into Eq. (16) and, after subtracting the mean of the resulting equation
 172 from Eq. (16), the result is the following equation describing the depth-averaged head
 173 perturbation

$$174 \quad \frac{S_s}{K} \frac{\partial}{\partial t} h'(x,t) = \frac{\partial^2}{\partial x^2} h'(x,t) + 2 \frac{\partial}{\partial x} \ln B(x) \frac{\partial}{\partial x} h'(x,t) + \frac{r(t)}{B(x)K}, \quad (17)$$

175 where $h'(x,t)$ is the fluctuations in depth-averaged head.

176 If it is assumed that the thickness of confined aquifer increases exponentially in
 177 x -direction in accordance with (Hantush, 1962; Marino and Luthin, 1982)

$$178 \quad B(x) = \beta e^{\alpha x}, \quad (18)$$

179 then Eq. (17) becomes

$$180 \quad \frac{S_s}{K} \frac{\partial}{\partial t} h'(x,t) = \frac{\partial^2}{\partial x^2} h'(x,t) + 2\alpha \frac{\partial}{\partial x} h'(x,t) + \frac{e^{-\alpha x}}{\beta K} r(t). \quad (19)$$

181 In Eq. (18), β and α are positive geometrical parameters. Furthermore, the outcrop (x
 182 = 0) and outlet ($x = L$) of the confined aquifer are considered as constant head
 183 boundaries. Since Eq. (19) only quantifies the response of the depth-averaged head to
 184 changes in the recharge rate, the initial and boundary conditions for Eq. (19) may be
 185 represented as follows

186 $h'(x,0;\omega) = 0,$ (20a)

187 $h'(0,t;\omega) = 0,$ (20b)

188 $h'(L,t;\omega) = 0.$ (20c)

189 The following Fourier-Stieltjes integral representation of a depth-averaged head

190 process is used to solve Eqs. (19) and (20) for the fluctuations h' in terms of r :

191 $h'(x,t) = \int_{-\infty}^{\infty} A_h(x,t;\omega) dZ_{\xi}(\omega),$ (21)

192 where A_h is the oscillatory function of depth-averaged head process. The resulting

193 differential equation for the oscillatory functions is found from using Eqs. (2) and (21)

194 in Eqs. (19) and (20) as

195 $\frac{S_s}{K} \frac{\partial}{\partial t} A_h(x,t;\omega) = \frac{\partial^2}{\partial x^2} A_h(x,t;\omega) + 2\alpha \frac{\partial}{\partial x} A_h(x,t;\omega) + \frac{e^{-\alpha x}}{\beta K} A_r(t;\omega).$ (22)

196 with the following conditions:

197 $A_h(x,0;\omega) = 0,$ (23a)

198 $A_h(0,t;\omega) = 0,$ (23b)

199 $A_h(L,t;\omega) = 0.$ (23c)

200 By solving the above boundary value problem, the oscillatory function of

201 depth-averaged head process is found to be (see Appendix A)

202 $A_h(x,t;\omega) = \frac{2}{S_s \beta} \sum_{n=1}^{n=\infty} \frac{1 - \cos(n\pi)}{n\pi} \exp(-\mu \frac{x}{L}) \sin(n\pi \frac{x}{L}) \int_0^t \exp[-\theta_n(t-\tau)] A_r(\tau;\omega) d\tau,$ (24)

203 where $\mu = \alpha L$ and $\theta_n = \overline{K} (n^2 \pi^2 + \mu^2) / (S_s L^2)$. It implies from Eqs. (3), (15) and (24) that

204 at the arbitrary location $x = x_\varepsilon$

205 $A_q(t; \omega) = A_{q_x}(x_\varepsilon, t; \omega)$

206
$$= -2 \frac{\bar{K}}{S_s L} \sum_{n=1}^{n=\infty} \frac{1 - \cos(n\pi)}{n\pi} [n\pi \cos(n\pi Y) - \mu \sin(n\pi Y)] \int_0^t \exp[-\theta_n(t - \tau)] A_r(\tau; \omega) d\tau, \quad (25)$$

207 where $Y = x_\varepsilon/L$. This means that the impulse response function of the system φ in Eqs.

208 (1) or (5) is taken in the form

209
$$\varphi(t, \tau) = -2 \frac{\bar{K}}{S_s L} \sum_{n=1}^{n=\infty} \frac{1 - \cos(n\pi)}{n\pi} [\cos(n\pi Y) - \mu \sin(n\pi Y)] \exp[-\theta_n(t - \tau)]. \quad (26)$$

210

211 **4 Results and discussion**

212

213 Equation (25) implies that the transfer function $|A_q|^2$ depends on the oscillatory

214 function of the temporal random rainfall process; consequently, to complete the

215 analysis of the transfer function the oscillatory function of the temporal random

216 rainfall process must be specified. It is assumed that the generated temporal random

217 perturbations of rainfall field are governed by the noise forced diffusive rainfall model

218 (North et al., 1993)

219
$$\tau_0 \frac{\partial}{\partial t} \rho(x, t) = \lambda_0^2 \frac{\partial^2}{\partial x^2} \rho(x, t) - \rho(x, t) + \xi(t), \quad (27)$$

220 where ρ is a zero-mean rainfall rate perturbation, τ_0 and λ_0 are the characteristic time

221 and length scales, respectively, which are inherent to the rainfall field, and ξ is a

222 zero-mean random stationary forcing process which has a spectral representation of

223 the form (e.g., Lumley and Panofsky, 1964)

$$224 \quad \xi(t) = \int_{-\infty}^{\infty} e^{i\omega t} dZ_{\xi}(\omega). \quad (28)$$

225 In Eq. (27), the rainfall-rate field is represented as a first-order continuous
226 autoregressive process in time and an isotropic second-order autoregressive process in
227 space.

228 Furthermore, the rest of this study takes into account that rain falls within a
229 defined period of time over a certain area of horizontal extension from $x = -\ell$ to $x = \ell$.

230 As such, the initial and boundary conditions for rainfall rate perturbations may be
231 represented by

$$232 \quad \rho(x, 0) = 0, \quad (29a)$$

$$233 \quad \rho(-\ell, t) = 0, \quad (29b)$$

$$234 \quad \rho(\ell, t) = 0. \quad (29c)$$

235

236 **4.1 Nonstationary random rainfall fields in time**

237

238 Using the Fourier-Stieltjes integral representation for the perturbation ρ ,

$$239 \quad \rho(x, t) = \int_{-\infty}^{\infty} A_{\rho}(x, t; \omega) dZ_{\xi}(\omega), \quad (30)$$

240 and Eq. (28) in Eq. (27), it follows that

241 $\tau_0 \frac{\partial}{\partial t} A_\rho(x, t; \omega) = \lambda_0^2 \frac{\partial^2}{\partial x^2} A_\rho(x, t; \omega) - A_\rho(x, t; \omega) + e^{i\omega t},$ (31)

242 where A_ρ is the oscillatory function of the rainfall rate processes. With the application

243 of the initial and boundary conditions,

244 $A_\rho(x, 0; \omega) = 0,$ (32a)

245 $A_\rho(-\ell, t; \omega) = 0,$ (32b)

246 $A_\rho(\ell, t; \omega) = 0,$ (32c)

247 the solution of Eqs. (31) and (32) is given by (see Appendix B)

248 $A_\rho(x, t; \omega) = 2 \sum_{m=1}^{m=\infty} \frac{1 - \cos(m\pi)}{m\pi} \sin(m\pi \frac{x + \ell}{2\ell}) \frac{\exp(i\Omega_t) - \exp(-\Theta_m t / \tau_0)}{\Theta_m + i\Gamma},$ (33)

249 where $\Theta_m = 1 + m^2 \pi^2 \eta^2$, $\eta = \lambda_0 / (2\ell)$, $\Omega_t = \omega t$, and $\Gamma = \omega \tau_0$.

250 In the case where the regional confined aquifer is directly recharged by rainfall at

251 the aquifer outcrop ($x = 0$), the oscillatory function is reduced to

252 $A_r(t; \omega) = A_\rho(0, t; \omega) = 2 \sum_{m=1}^{m=\infty} \frac{1 - \cos(m\pi)}{m\pi} \sin(m \frac{\pi}{2}) \frac{\exp(i\Omega_t) - \exp(-\Theta_m t / \tau_0)}{\Theta_m + i\Gamma}.$ (34)

253 Correspondingly, the power spectrum of rainfall rate, $S_{rr}(t, \omega)$, can be expressed by

254 $S_{rr}(t; \omega) = |A_r(t; \omega)|^2 S_{\xi\xi}(\omega)$

255 $= 4 \sum_{n=1}^{n=\infty} \sum_{m=1}^{m=\infty} \frac{1 - \cos(m\pi)}{m\pi} \frac{1 - \cos(n\pi)}{n\pi} \sin(m \frac{\pi}{2}) \sin(n \frac{\pi}{2}) \frac{1}{\Theta_m^2 + \Gamma^2} \frac{1}{\Theta_n^2 + \Gamma^2}$

256 $\left\{ (\Theta_m \Theta_n + \Gamma^2) [1 + T_1 - T_2 \cos(\Omega_t)] - T_3 \Gamma (\Theta_m - \Theta_n) \sin(\Omega_t) \right\} S_{\xi\xi}(\omega),$ (35)

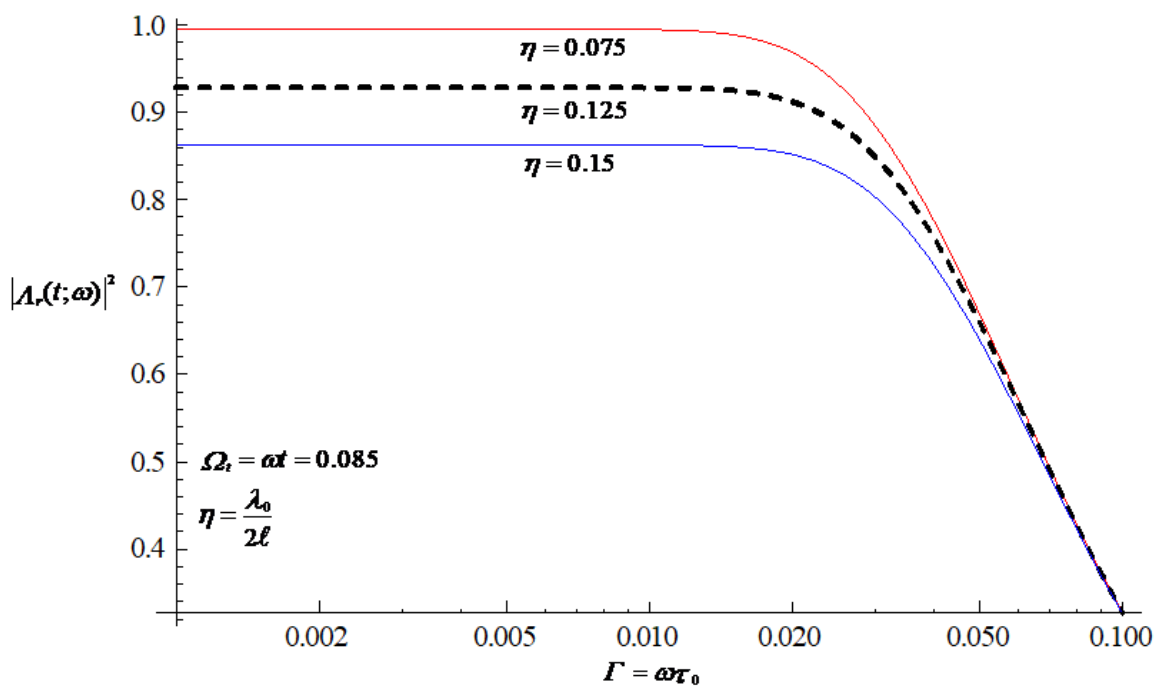
257 where $T_1 = \exp[-(\Theta_m + \Theta_n)t / \tau_0]$, $T_2 = \exp(-\Theta_m t / \tau_0) + \exp(-\Theta_n t / \tau_0)$, and $T_3 =$

258 $\exp(-\Theta_m t / \tau_0) - \exp(-\Theta_n t / \tau_0)$.

259 The transfer function of the rainfall processes in Eq. (35) behaves like a filter,

260 attenuating the high-frequency part of the rainfall spectrum. The graph of transfer
 261 function, which is characterized by the characteristic time scale τ_0 for different
 262 characteristic length scales, is shown in Fig. 2. It clearly shows a reduction of the
 263 transfer function with increasing τ_0 , implying a reduction of the variability of the
 264 rainfall field with the characteristic time scale of the rainfall field. A larger τ_0
 265 decreases the temporal persistence of the rainfall fluctuations, resulting in a smaller
 266 transfer function. It is also seen that for a fixed value of the time scale, the transfer
 267 function of the rainfall processes tends to decrease as the length scale of the rainfall
 268 field increases. The influence of the length scale plays a similar role as the influence
 269 of the time scale in reducing the temporal persistence of the rainfall fluctuations and
 270 thus the variability of the rainfall field.

271



273 **Figure 2.** Graphical representation of the transfer function of the rainfall processes in
 274 Eq. (35) characterized by the time scale for different length scales, where the series
 275 calculation is truncated up to $M = N = 100$.

276 Through the use of Eq. (25) and Eq. (34), the oscillatory function of the
 277 integrated discharge process could be represented as follows:

$$\begin{aligned}
 278 \quad A_q(t; \omega) = & -4 \frac{\bar{K}}{S_s L} \sum_{n=1}^{n=\infty} \frac{1 - \cos(n\pi)}{n\pi} [n\pi \cos(n\pi\gamma) - \mu \sin(n\pi\gamma)] \\
 279 \quad & \times \sum_{m=1}^{m=\infty} \frac{1 - \cos(m\pi)}{m\pi} \frac{\sin(m\frac{\pi}{2})}{\Theta_m + i\Gamma} \left[\frac{\exp(i\Omega_t) - \exp(-\theta_n t)}{\theta_n + i\omega} - \frac{\exp(-\Theta_m t / \tau_0) - \exp(-\theta_n t)}{\theta_n - \Theta_m / \tau_0} \right].
 \end{aligned}$$

(36)

281 Thus, the transfer function of the integrated discharge flux is taken in the form

$$\begin{aligned}
 282 \quad \frac{S_{qq}(t; \omega)}{S_{\xi\xi}(\omega)} = & |A_q(t; \omega)|^2 = 16L^2 \mathcal{G}^2 \left\{ \left[\sum_{n=1}^{n=\infty} \sum_{m=1}^{m=\infty} \Psi_1 \Psi_2 \left(\frac{\Theta_m \Psi_3 + \Gamma \Psi_4}{\theta_n^2 \tau_0^2 + \Gamma^2} + \frac{\Theta_m \Psi_5}{\Theta_m - \theta_n \tau_0} \right) \right]^2 \right. \\
 283 \quad & \left. + \left[\sum_{n=1}^{n=\infty} \sum_{m=1}^{m=\infty} \Psi_1 \Psi_2 \left(\frac{\Theta_m \Psi_4 - \Gamma \Psi_3}{\theta_n^2 \tau_0^2 + \Gamma^2} - \frac{\Gamma \Psi_5}{\Theta_m - \theta_n \tau_0} \right) \right]^2 \right\},
 \end{aligned}$$

(37)

284 where $\mathcal{G} = \bar{K} \tau_0 / (S_s L^2)$ and

$$285 \quad \Psi_1 = \frac{1}{\Theta_m^2 + \Gamma^2} \frac{1 - \cos(m\pi)}{m\pi} \sin(m\frac{\pi}{2}), \tag{38a}$$

$$286 \quad \Psi_2 = \frac{1 - \cos(n\pi)}{n\pi} [\cos(n\pi\gamma) - \mu \sin(n\pi\gamma)], \tag{38b}$$

$$287 \quad \Psi_3 = \Gamma \sin(\Omega_t) + \theta_n \tau_0 [\cos(\Omega_t) - \exp(-\theta_n t)], \tag{38c}$$

$$288 \quad \Psi_4 = \theta_n \tau_0 \sin(\Omega_t) - \Gamma [\cos(\Omega_t) - \exp(-\theta_n t)], \tag{38d}$$

$$289 \quad \Psi_5 = \exp(-\Theta_m t / \tau_0) - \exp(-\theta_n t). \tag{38e}$$

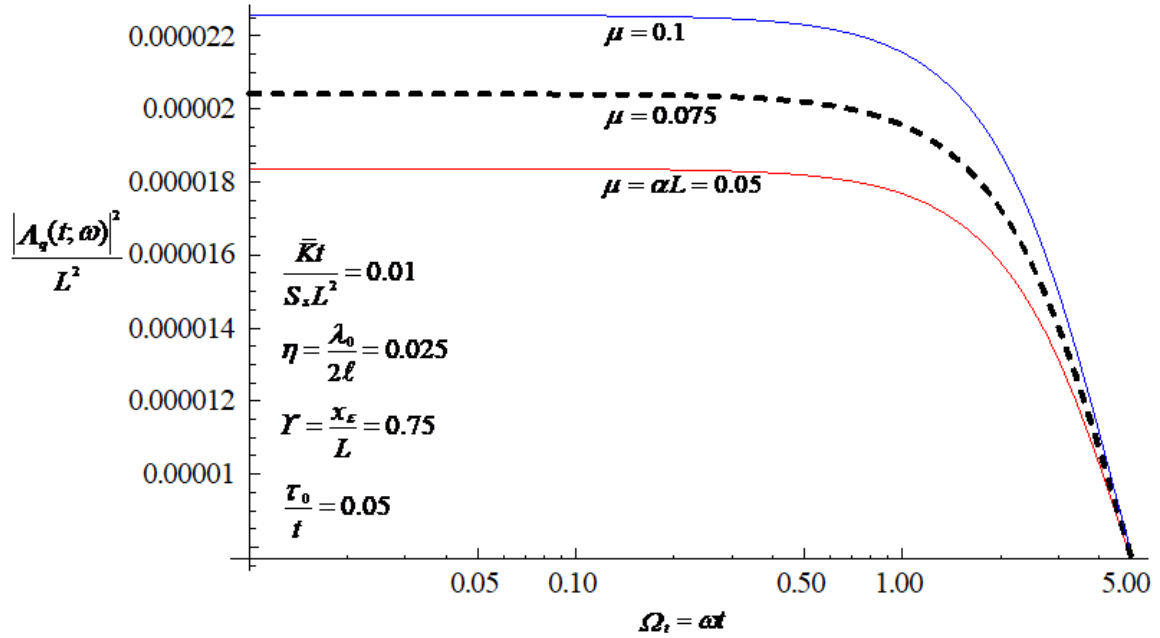
290 Note that the linearity in modeling the recharge-discharge response of a
 291 catchment in Eq. (1), which was originally developed for large catchments, increases

292 with catchment area (e.g., Chow et al., 1988). This implies that the impulse responses
293 and transfer functions derived here are valid in large confined aquifers.

294 An essential feature of the transfer function of the integrated discharge flux in Eq.
295 (37) is the resulting filtering associated with the flow process, as shown in Fig. 3. The
296 attenuating the high-frequency part of the flow discharge spectrum means that the
297 flow process smooths-out much of the small-scale variations caused by the rainfall
298 field. Physically, this feature implies that the flow field is much smoother than the
299 rainfall field. The figure also shows that the transfer function at fixed values for
300 frequency and time increases with the increasing thickness of the confined aquifer. An
301 increase in the thickness of the aquifer leads to an increased temporal persistence of
302 the flow discharge fluctuations caused by the variation of the rainfall field and thus to
303 an increase in the variability of integrated discharge field. As shown in Fig. 4, the
304 ratio of the mean hydraulic conductivity to the storage coefficient (often referred to as
305 the aquifer diffusivity) plays a similar role in influencing the variation of the transfer
306 function as the thickness of the confined aquifer. The introduction of a larger aquifer
307 diffusivity leads to a larger transfer function of integrated discharge and thus to a
308 larger variability of the discharge field. Since the variability of the discharge field is
309 positively correlated with that of rainfall field, the variability of the integrated
310 discharge field will decrease with increasing characteristic time or length scale of the

311 rainfall field (see Fig. 2).

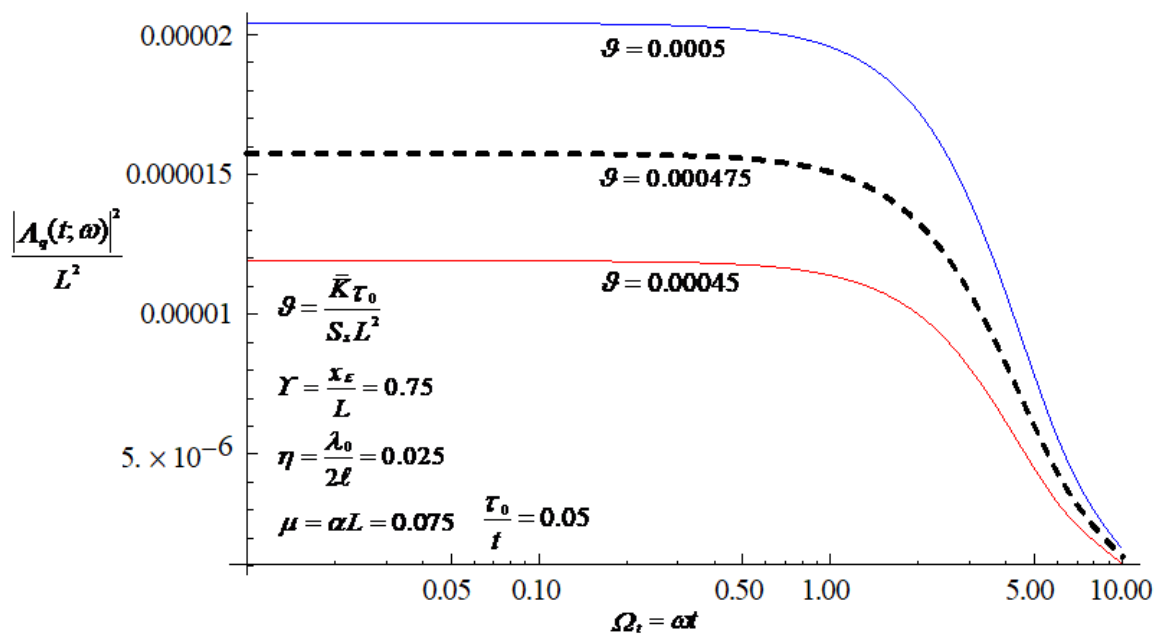
312



314 **Figure 3.** Influence of the thickness of the confined aquifer on the transfer function of

315 the discharge flux, where the series calculation is truncated up to $M = N = 100$.

316



318 **Figure 4.** Influence of the aquifer diffusivity on the transfer function of the discharge
 319 flux, where the series calculation is truncated up to $M = N = 100$.

320 From Eqs. (4) or (8), the transfer function can be defined as the ratio of the
 321 fluctuations of an observation of output time series to those of input time series in
 322 frequency domain. Equations (35) and (37) indicate that the transfer functions are
 323 related to the properties of the rainfall field and the aquifer, such as the characteristic
 324 scales of time and length of rainfall field and the diffusivity and thickness parameters
 325 of the aquifer. Therefore, the transfer function derived here has the potential to
 326 perform a parameter estimation based on the observations of input and output time
 327 series using the inverse modeling approach.

328 The traditional approach to regional groundwater flow problems introduces the
 329 transmissivity term, the depth-integrated hydraulic conductivity operator

$$330 \quad T(x_1, x_2) = \int_{b_1(x_1, x_2)}^{b_2(x_1, x_2)} K(x_1, x_2, x_3) dx_3 \quad (39)$$

331 into to the groundwater flow equation (diffusion equation) to reduce the
 332 three-dimensional equation to a two-dimensional one:

$$333 \quad S(x_1, x_2) \frac{\partial}{\partial t} h(x_1, x_2, t) = \frac{\partial}{\partial x_i} [T(x_1, x_2) \frac{\partial}{\partial x_i} h(x_1, x_2, t)] \quad i = 1, 2 \quad (40)$$

334 This means that the effects of both the variation of K in x_3 -direction and the aquifer
 335 thickness are implicitly reflected in the term $T(x_1, x_2)$. This leads to great difficulties in

336 assessing the influence of aquifer thickness on the flow field with Eq. (40).

337 The proposed diffusion equation of this work,

$$338 \quad S_s(x_1, x_2) \frac{\partial \tilde{h}(x_1, x_2, t)}{\partial x_i} = \frac{1}{B(x_1, x_2)} \frac{\partial}{\partial x_i} \left[K(x_1, x_2) B(x_1, x_2) \frac{\partial \tilde{h}(x_1, x_2, t)}{\partial x_i} \right] + K(x_1, x_2) \frac{\partial \ln B(x_1, x_2)}{\partial x_i} \frac{\partial \tilde{h}(x_1, x_2, t)}{\partial x_i} \quad i=1,2$$

339 (41)

340 derived by the hydraulic approach (Bear, 1979; Bear and Cheng, 2010), provides an
341 efficient way to analyze flow fields in confined aquifers of non-uniform thickness.

342 Note that Eq. (41) is the reformulation of Eq. (11). In addition, the usual observations
343 of flow in porous media are measurements of hydraulic head from wells screened
344 over extended sections of the medium. The measurement at a given location
345 approximately represents a depth-averaged actual hydraulic head resulting from flow
346 through a three-dimensional hydraulic conductivity field across the thickness of the
347 medium. This means that the depth-averaged head representation used in Eq. (41) is
348 consistent with what is observed in the fields.

349 Climate changes have a direct influence on the rainfall event (e.g., Trenberth, 2011;
350 Pendergrass et al., 2014; Eekhout et al., 2018). The nonstationarity in the statistical
351 properties of rainfall field is a representation of climate change (e.g., Razavi et al.,
352 2015; López and Francés, 2013; Benoit et al., 2020). The nonstationary effect of
353 climatic change over time on variability of groundwater specific discharge has not yet
354 been well characterized in the. The transfer function in Eq. (37), which relates the

355 nonstationary spectra of the rainfall fluctuations to those of integrated discharge
 356 variation, generalizes existing studies that considered stationary recharge/discharge
 357 fields. To our knowledge, it has not been previously presented in the literature and has
 358 the potential to analyze the effects of climate change on temporal groundwater
 359 specific discharge variability.

360

361 **4.2 Application in the prediction of outflow discharge**

362

363 The usefulness of the stochastic theory presented here lies in its essentially predictive
 364 nature. The variance can be used as a quantification of the uncertainty associated with
 365 the prediction in field situations using the linear system model. In this sense, the
 366 solution of Eq. (1) \pm two times the square root of the variance provides a rational
 367 framework for predicting discharge over a relatively large spatial scale where direct
 368 observations of such a dependent variable are not possible.

369 For large times, the first term in Eq. (37) dominates the sum of the other terms,

370 and therefore the transfer function can be approximated by

$$\begin{aligned}
 371 \quad |A_q(t; \omega)|^2 &= \frac{256}{\pi^2} L^2 g^2 [\pi \cos(\pi \gamma) - \mu \sin(\pi \gamma)]^2 \frac{1}{\Theta_i^2 + \Gamma^2} \\
 372 \quad &\left\{ \Xi^2 + \frac{1}{\forall^2 + \Gamma^2} [1 + 2\forall \Xi T_A + T_A^2 - 2(\forall \Xi + T_A) \cos(\Omega_i) - 2\Xi \Gamma \sin(\Omega_i)] \right\} \quad (42)
 \end{aligned}$$

373 where $\Theta_i = 1 + \pi^2 \eta^2$, $\forall = \overline{K} \tau_0 (\pi^2 + \mu^2) / (S_s L^2)$, $\Xi = (T_R - T_A) / (\forall - \Theta_i)$, $T_R = \exp(-\Theta_i t / \tau_0)$, and

374 $T_A = \exp(-\forall t/\tau_0)$. If the variation of the rainfall event is generated by a random white
 375 noise forcing, the variance of the outflow discharge at large times can then be
 376 calculated using Eq. (42) as

$$\begin{aligned}
 377 \quad \sigma_q^2(t) &= \int_{-\infty}^{\infty} S_{qq}(t; \omega) d\omega = \int_{-\infty}^{\infty} |A_q(t; \omega)|^2 S_{\xi\xi}(\omega) d\omega \\
 378 \quad &= \frac{256}{\pi} \frac{G_0 L^2}{\tau_0} g^2 [\pi \cos(\pi\gamma) - \mu \sin(\pi\gamma)]^2 \left\{ \frac{\Xi^2}{\Theta_1} + \frac{1 + 2\forall\Xi T_A + T_A^2}{\forall\Theta_1(\forall + \Theta_1)} \right. \\
 379 \quad &\quad \left. - 2(\forall\Xi + T_A) \frac{\Theta_1 T_A - \forall T_R}{\forall\Theta_1(\Theta_1^2 - \forall^2)} - 2\Xi \frac{T_R - T_A}{\Theta_1^2 - \forall^2} \right\}, \quad (43)
 \end{aligned}$$

380 where G_0 represents a constant spectral density of a white noise process. Note that
 381 white noise is a signal that contains all frequencies in equal proportions, that is, a
 382 signal whose spectrum is flat.

383 After observing the recharge rate $R(t)$ over time at the outcrop of the aquifer and
 384 identifying input parameters such as the specific storage coefficient, mean hydraulic
 385 conductivity and geometrical parameters of the aquifer and the characteristic time and
 386 length scales of the rainfall event for a given area or region, the discharge can be
 387 determined under uncertainty in the far downstream aquifer area, Eq. (1) together with
 388 Eq. (26) \pm two times the square root of Eq. (43). It provides an important basis for the
 389 rational management of regional groundwater resources in complex geologic settings
 390 under uncertainty.

391

392 **4.3 A note on stationary random rainfall fields in time**

393

394 If the temporal random rainfall fields are stationary, there exists a representation of
 395 the rainfall perturbation process in terms of a Fourier-Stieltjes integral as Eq. (6).

396 Substituting Eqs. (6) and (21) into Eq. (19) gives

$$397 \quad \frac{S_s}{K} \frac{\partial}{\partial t} A_h(x, t; \omega) = \frac{\partial^2}{\partial x^2} A_h(x, t; \omega) + 2\alpha \frac{\partial}{\partial x} A_h(x, t; \omega) + \frac{e^{-\alpha x}}{\beta K} e^{i\omega t}. \quad (44)$$

398 The solution of Eq. (44) with conditions Eq. (23) is

$$399 \quad A_h(x, t; \omega) = \frac{2}{S_s \beta} \sum_{n=1}^{n=\infty} \frac{1 - \cos(n\pi)}{n\pi} \exp\left(-\mu \frac{x}{L}\right) \sin\left(n\pi \frac{x}{L}\right) \frac{\exp(i\Omega_t) - \exp(-\theta_n t)}{\theta_n + i\omega}, \quad (45)$$

400 so that

$$401 \quad A_q(t; \omega) = -2 \frac{\bar{K}}{S_s L} \sum_{n=1}^{n=\infty} \frac{1 - \cos(n\pi)}{n\pi} [n\pi \cos(n\pi\gamma) - \mu \sin(n\pi\gamma)] \frac{\exp(i\Omega_t) - \exp(-\theta_n t)}{\theta_n + i\omega}. \quad (46)$$

402 and thus

$$403 \quad |A_q(t; \omega)|^2 = 4L^2 \bar{K}^2 \sum_{n=1}^{n=\infty} \sum_{m=1}^{m=\infty} \frac{\Phi(m)\Phi(n)}{(\theta_n^2 \tau_0^2 + \Gamma^2)(\theta_m^2 \tau_0^2 + \Gamma^2)} [(\theta_m \theta_n \tau_0^2 + \Gamma^2)(1 + \Delta_1 - \cos(\Omega_t) \Delta_2) - \Gamma \sin(\Omega_t)(\theta_m - \theta_n) \tau_0 \Delta_3],$$

404 (47)

405 where

$$406 \quad \Phi(y) = \frac{1 - \cos(y\pi)}{y\pi} [y\pi \cos(y\pi\gamma) - \mu \sin(y\pi\gamma)], \quad (48)$$

$$407 \quad \Delta_1 = \exp[-(\theta_m + \theta_n)t], \Delta_2 = \exp(-\theta_m t) + \exp(-\theta_n t), \text{ and } \Delta_3 = \exp(-\theta_m t) - \exp(-\theta_n t).$$

408 At large times, Eq. (35) approach a finite value as

$$409 \quad S_{rr}(\omega) = 4 \sum_{n=1}^{n=\infty} \sum_{m=1}^{m=\infty} \frac{1 - \cos(m\pi)}{m\pi} \frac{1 - \cos(n\pi)}{n\pi} \sin\left(m \frac{\pi}{2}\right) \sin\left(n \frac{\pi}{2}\right) \frac{\theta_m \theta_n + \Gamma^2}{(\theta_m^2 + \Gamma^2)(\theta_n^2 + \Gamma^2)} S_{\xi\xi}(\omega). \quad (49)$$

410 and the corresponding rainfall process is stationary. Combining Eq. (47) with Eq. (49)

411 gives

$$\begin{aligned}
412 \quad \frac{S_{qq}(\omega)}{S_{\xi\xi}(\omega)} &= 16L^2 \mathcal{G}^2 \left\{ \sum_{n=1}^{n=\infty} \sum_{m=1}^{m=\infty} \frac{\Phi(m)\Phi(n)}{(\theta_n^2 \tau_0^2 + \Gamma^2)(\theta_m^2 \tau_0^2 + \Gamma^2)} \left[(\theta_m \theta_n \tau_0^2 + \Gamma^2)(1 + \Delta_1 - \cos(\Omega_t) \Delta_2) - \Gamma \sin(\Omega_t)(\theta_m - \theta_n) \tau_0 \Delta_3 \right] \right\} \\
413 \quad &\times \left[\sum_{n=1}^{n=\infty} \sum_{m=1}^{m=\infty} \frac{1 - \cos(m\pi)}{m\pi} \frac{1 - \cos(n\pi)}{n\pi} \sin\left(m \frac{\pi}{2}\right) \sin\left(n \frac{\pi}{2}\right) \frac{\Theta_m \Theta_n + \Gamma^2}{(\Theta_m^2 + \Gamma^2)(\Theta_n^2 + \Gamma^2)} \right]. \quad (50)
\end{aligned}$$

414 Note that the nonstationarity in the hydraulic head or integrated discharge is
415 introduced by a nonuniform thickness of the confined aquifer, even if the recharge
416 field is stationary. Nonuniformity in the mean flow, for example, can also cause the
417 nonstationarity in the statistics of random flow fields in heterogeneous aquifers (e.g.,
418 Rubin and Bellin, 1994; Ni and Li, 2006; Ni et al., 2010).

419

420 5 Conclusions

421

422 An analytical transfer function is developed to describe the spectral response
423 characteristics of confined aquifers with variable thickness to the variation of the
424 rainfall field, where the aquifer is directly recharged by rainfall at the outcrop of the
425 aquifer. The rainfall-discharge process is treated as nonstationary in time, as it reflects
426 the stochastic nature of the hydrological process. Any varying rainfall input at any
427 time resolution can be convolved with the transfer function (or impulse response
428 function) to simulate any discharge output of a linear model. The transfer function
429 derived here, which relates the nonstationary spectra of the rainfall fluctuations to
430 those of integrated discharge variation, has the potential to analyze the influence of

431 climate change on groundwater recharge variability.

432 The closed-form results of this work are developed on the basis of the
433 Fourier-Stieltjes representation approach, which allows to analyze the effects of the
434 controlling parameters in the models on the transfer function of the integrated
435 discharge. It is founded that the persistence of rainfall fluctuations is greater for a
436 smaller value of the characteristic time or length scale of the rainfall field, which in
437 turn leads to greater variability of the integrated discharge field. The attenuating
438 characteristic of the confined aquifer flow system is observed in the spectral domain.
439 The variability of the integrated discharge in confined aquifer with variable thickness
440 is increased with the thickness parameter α . The larger the aquifer diffusivity, the
441 greater the spectrum (variability) of the integrated discharge.

442

443 **Appendix A: Evaluation of \mathcal{A}_h in Eq. (20)**

444

445 The boundary-value problem describing the depth-averaged head fluctuations induced
446 by the variation of recharge rate in frequency domain is given by Eqs. (22) and (23).

447 Using the transformation,

$$448 \mathcal{A}_h(x, t; \omega) = \exp\left[-\alpha\left(x + \frac{\alpha \bar{K}}{S_s} t\right)\right] U(x, t; \omega), \quad (\text{A1})$$

449 Eq. (22) in $\mathcal{A}_h(x, t; \omega)$ together with Eq. (23) can be converted into a new (easier) one

450 in a new variable $U(x,t;\omega)$ as

$$451 \quad \frac{\partial}{\partial t}U(x,t;\omega) = \frac{\bar{K}}{S_s} \frac{\partial^2}{\partial x^2}U(x,t;\omega) + \frac{1}{\beta S_s} \exp\left(\frac{\bar{K}\alpha^2}{S_s}t\right)A_r(t;\omega), \quad (\text{A2})$$

452 with

$$453 \quad U(x,0;\omega) = 0, \quad (\text{A3a})$$

$$454 \quad U(0,t;\omega) = 0, \quad (\text{A3b})$$

$$455 \quad U(L,t;\omega) = 0. \quad (\text{A3c})$$

456 The solution of Eqs. (A2) and (A3) can be found by the technique of separation of

457 variables (e.g., Farlow, 1993) as

$$458 \quad U(x,t;\omega) = \frac{2}{S_s\beta} \sum_{n=1}^{\infty} \frac{1 - \cos(n\pi)}{n\pi} \sin\left(n\pi \frac{x}{L}\right) \int_0^t \exp[-\nu_n(t-\tau)] \exp\left(\frac{\bar{K}}{S_s}\alpha^2\tau\right) A_r(\tau;\omega) d\tau, \quad (\text{A4})$$

459 where $\nu_n = \bar{K}n^2\pi^2/(S_sL^2)$. With reference to Eq. (A1), the solution of Eqs. (22) and (23)

460 is then given by Eq. (24).

461

462 **Appendix B: Evaluation of A_p in Eq. (31)**

463

464 Making use of the transformation,

$$465 \quad A_p(x,t;\omega) = \exp\left(-\frac{t}{\tau_0}\right)u(x,t;\omega), \quad (\text{B1})$$

466 leads Eqs. (31) and (32) to

$$467 \quad \frac{\partial}{\partial t}u(x,t;\omega) = \frac{\lambda_0^2}{\tau_0} \frac{\partial^2}{\partial x^2}u(x,t;\omega) + \frac{1}{\tau_0} \exp\left[\left(\frac{1}{\tau_0} + i\omega\right)t\right], \quad (\text{B2})$$

468 with

469 $u(x, 0; \omega) = 0,$ (B3a)

470 $u(-\ell, t; \omega) = 0,$ (B3b)

471 $u(\ell, t; \omega) = 0.$ (B3c)

472 In a similar way, based on the technique of separation of variables, Eqs. (B2) and (B3)

473 arrive at the solution in the form

474
$$u(x, t; \omega) = 2 \sum_{m=1}^{m=\infty} \frac{1 - \cos(m\pi)}{m\pi} \sin\left(m\pi \frac{x + \ell}{2\ell}\right) \frac{\exp[(1 + i\Gamma)t / \tau_0] - \exp(-\zeta_m t / \tau_0)}{\Theta_m + i\Gamma},$$
 (B4)

475 where $\zeta_m = m^2 \pi^2 \eta^2$, $\eta = \lambda_0 / (2\ell)$, $\Theta_m = 1 + \zeta_m$, and $\Gamma = \omega \tau_0$. The use of Eqs. (B1) and (B4)

476 results in Eq. (33).

477

478 *Data availability.* No data was used for the research described in the article.

479

480 *Author contributions.* C-MC: Conceptualization, Methodology, Formal analysis,

481 Writing - original draft preparation, Writing - review & editing.

482 C-FN: Conceptualization, Methodology, Formal analysis, Writing - original draft

483 preparation, Writing - review & editing, Supervision, Funding acquisition.

484 W-CL: Conceptualization, Methodology, Formal analysis, Writing - original draft

485 preparation, Writing - review & editing.

486 C-PL: Conceptualization, Methodology, Formal analysis, Writing - original draft

487 preparation, Writing - review & editing.

488 I-HL: Conceptualization, Methodology, Formal analysis, Writing - original draft

489 preparation, Writing - review & editing.

490

491 *Competing interests.* The authors declare that they have no conflict of interest.

492

493 *Acknowledgements.* Research leading to this paper has been partially supported by the

494 grant from the Taiwan Ministry of Science and Technology under the grants MOST

495 108-2638-E-008-001-MY2, MOST 108-2625-M-008 -007, and MOST

496 107-2116-M-008 -003 -MY2. We are grateful to the Editor Prof. Nadia Ursino and

497 anonymous referees for constructive comments that improved the quality of the work.

498

499 **References**

500

501 Bear, J.: Hydraulics of groundwater, McGraw-Hill, New York, 1979.

502 Bear, J. and Cheng, A.H.-D.: Modeling groundwater flow and contaminant transport,

503 Springer, Dordrecht, 2010.

504 Benoit, L., Vrac, M., and Mariethoz, G.: Nonstationary stochastic rain type generation:

505 accounting for climate drivers, Hydrol. Earth Syst. Sci., 24(5), 2841-2854, 2020.

506 Christensen, N. S. and Lettenmaier, D. P.: A multimodel ensemble approach to

507 assessment of climate change impacts on the hydrology and water resources of

508 the Colorado River Basin, Hydrol. Earth Syst. Sci., 11(4), 1417-1434, 2007.

509 Chow, V. T., Maidment, D. R., and Mays, L. W.: Applied hydrology, McGraw-Hill,

510 1988.

511 Cooper, H. H. and Rorabaugh, M.J.: Ground water movements and bank storage due
512 to flood stages in surface streams, USGS Water Supply Paper 1536-J. Reston,
513 Virginia: USGS, 1963.

514 de Marsily, G.: Quantitative hydrogeology: Groundwater hydrology for engineers,
515 Academic Press, Orlando, FL, 1986.

516 Eekhout, J. P. C., Hunink, J. E., Terink, W., and de Vente, J.: Why increased extreme
517 precipitation under climate change negatively affects water security, *Hydrol.*
518 *Earth Syst. Sci.*, 22(11), 5935-5946, 2018.

519 Farlow, S. J.: Partial differential equations for scientists and engineers, Dover, New
520 York, N. Y., 1993.

521 Gelhar, L. W.: Stochastic analysis of phreatic aquifer, *Water Resour. Res.*, 10(3),
522 539-545, 1974.

523 Hantush, M.S.: Flow of ground water in sands of nonuniform thickness: 3. Flow to
524 wells, *J. Geophys. Res.*, 67(4), 1527-1534, 1962.

525 Long, A. J. and Mahler, B. J.: Prediction, time variance, and classification of
526 hydraulic response to recharge in two karst aquifers, *Hydrol. Earth Syst. Sci.*,
527 17(1), 281-294, 2013.

528 López, J. and Francés, F.: Non-stationary flood frequency analysis in continental

529 Spanish rivers, using climate and reservoir indices as external covariates, *Hydrol.*
530 *Earth Syst. Sci.*, 17(8), 3189-3203, 2013

531 Lumley, J. L. and Panofsky, H. A.: *The structure of atmospheric turbulence*, John
532 Wiley, New York, 1964.

533 Marino, M. A. and Luthin, J. N.: *Seepage and Groundwater*, Elsevier, New York,
534 1982.

535 Milly, P. C. D., Betancourt, J., Falkenmark, M., Hirsch, R. M., Kundzewicz, Z. W.,
536 Lettenmaier, D. P., and Stouffer, R. J.: Stationarity is Dead: Whither water
537 management? *Science*, 319(5863), 573-574, 2008.

538 Molénat, J., Davy, P., Gascuel-Oudou, C., and Durand, P.: Study of three subsurface
539 hydrological systems based on spectral and cross-spectral analysis of time series,
540 *J. of Hydrol.*, 222(1-4), 152-164, 1999.

541 Ni, C.-F. and Li, S.-G.: Modeling groundwater velocity uncertainty in nonstationary
542 composite porous media, *Adv. Water Resour.*, 29(12), 1866-1875, 2006.

543 Ni, C.-F., Li, S.-G., Liu, C.-J., and Hsu, S. M.: Efficient conceptual framework to
544 quantify flow uncertainty in large-scale, highly nonstationary groundwater
545 systems, *J. Hydrol.*, 381(3-4), 297-307, 2010.

546 North, G. R., Shen, S. S. P., and Upson, R. B.: Sampling errors in rainfall estimates by
547 multiple satellites, *J. Appl. Meteor.*, 32(2), 399-410, 1993.

- 548 Olsthoorn, T.: Do a bit more with convolution, *Groundwater*, 46(1), 13-22, 2007.
- 549 Onder, H.: One-dimensional transient flow in a finite fractured aquifer system, *Hydrol.*
550 *Sci. J.*, 43(2), 243-265, 1998.
- 551 Pedretti, D., Russian, A., Sanchez-Vila, X., and Dentz, M.: Scale dependence of the
552 hydraulic properties of a fractured aquifer estimated using transfer functions,
553 *Water Resour. Res.*, 52(7), 5008-5024, 2016.
- 554 Pendergrass, A. G. and Hartmann, D. L.: Changes in the distribution of rain frequency
555 and intensity in response to global warming, *J. Clim.*, 27(22), 8372-8383, 2014.
- 556 Priestley, M. B.: Evolutionary spectra and non-stationary processes, *J. R. Stat. Soc. Ser.*
557 *B.*, 27(2), 204-237, 1965.
- 558 Razavi, S., Elshorbagy, A., Wheeler, H., and Sauchyn, D.: Toward understanding
559 nonstationarity in climate and hydrology through tree ring proxy records, *Water*
560 *Resour. Res.*, 51(3), 1813-1830, 2015.
- 561 Rinaldo, A. and Marani, A.: Basin scale model of solute transport, *Water Resour.*
562 *Res.*, 23(11), 2107-2118, 1987.
- 563 Rubin, Y. and Bellin, A.: The effects of recharge on flow nonuniformity and
564 macrodispersion, *Water Resour. Res.*, 30(4), 939-948, 1994.
- 565 Rugh, W. J.: *Nonlinear system theory: the Volterra/Wiener approach*, Johns Hopkins
566 University Press, Baltimore, 1981.

567 Russian, A., Dentz, M., Le Borgne, T., Carrera, J., and Jimenez-Martinez, J.: Temporal
568 scaling of groundwater discharge in dual and multicontinuum catchment models,
569 Water Resour. Res., 49(12), 8552-8564, 2013.

570 Sang, Y.-F., Sun, F., Singh, V. P., Xie, P., and Sun, J.: A discrete wavelet spectrum
571 approach for identifying non-monotonic trends in hydroclimate data, Hydrol.
572 Earth Syst. Sci., 22(1), 757-766, 2018.

573 Trenberth, K.: Changes in precipitation with climate change, Clim. Res., 47(1),
574 123-138, 2011.

575

576 **Figure captions**

577

578 **Figure 1.** Schematic representation of a linear block-box system.

579 **Figure 2.** Graphical representation of the transfer function of the rainfall processes in
580 Eq. (35) characterized by the time scale for different length scales, where the series
581 calculation is truncated up to $M = N = 100$.

582 **Figure 3.** Influence of the thickness of the confined aquifer on the transfer function of
583 the discharge flux, where the series calculation is truncated up to $M = N = 100$.

584 **Figure 4.** Influence of the aquifer diffusivity on the transfer function of the discharge
585 flux, where the series calculation is truncated up to $M = N = 100$.

586